

Training Deep Stereo Matching Networks on Tree Branch Imagery: A Benchmark Study for Real-Time UAV Forestry Applications

Yida Lin, Bing Xue, Mengjie Zhang

Centre for Data Science and Artificial Intelligence

Victoria University of Wellington, Wellington, New Zealand

linyida@myvuw.ac.nz, bing.xue@vuw.ac.nz, mengjie.zhang@vuw.ac.nz

Sam Schofield, Richard Green

Department of Computer Science and Software Engineering

University of Canterbury, Canterbury, New Zealand

sam.schofield@canterbury.ac.nz, richard.green@canterbury.ac.nz

Abstract—Autonomous drone-based tree pruning needs accurate, real-time depth estimation from stereo cameras. Depth is computed from disparity maps using $Z = fB/d$, so even small disparity errors cause noticeable depth mistakes at working distances. Building on our earlier work that identified DEFOM-Stereo as the best reference disparity generator for vegetation scenes, we present the first study to train and test ten deep stereo matching networks on real tree branch images. We use the Canterbury Tree Branches dataset—5,313 stereo pairs from a ZED Mini camera at 1080P and 720P—with DEFOM-generated disparity maps as training targets. The ten methods cover step-by-step refinement, 3D convolution, edge-aware attention, and lightweight designs. Using perceptual metrics (SSIM, LPIPS, ViTScore) and structural metrics (SIFT/ORB feature matching), we find that BANet-3D produces the best overall quality (SSIM=0.883, LPIPS=0.157), while RAFT-Stereo scores highest on scene-level understanding (ViTScore=0.799). Testing on an NVIDIA Jetson Orin Super (16 GB, independently powered) mounted on our drone shows that AnyNet reaches 6.99 FPS at 1080P—the only near-real-time option—while BANet-2D gives the best quality-speed balance at 1.21 FPS. We also compare 720P and 1080P processing times to guide resolution choices for forestry drone systems.

Index Terms—Stereo matching, disparity estimation, depth estimation, deep learning, UAV forestry, real-time inference, autonomous pruning

I. INTRODUCTION

Radiata pine (*Pinus radiata*) is the main plantation tree in New Zealand, where forestry adds NZ\$3.6 billion (1.3%) to the national economy. Trees need regular pruning to produce high-quality wood, but pruning by hand is dangerous due to fall risks and chainsaw injuries. Drones that prune automatically [1], [2] offer a safer option, yet they need centimeter-level depth accuracy to position cutting tools at 1–2 m distances. In a stereo camera system, depth is not measured directly. Instead, it comes from *disparity maps*—images that record how far each pixel shifts horizontally between the left and right camera views. Forest scenes are much harder than city or indoor environments because they contain thin overlapping branches, repeating textures, sharp depth changes, and large lighting differences. These challenges require training on vegetation-specific data rather than using general-purpose pretrained models.

Disparity Maps and Depth Recovery. A disparity map $D \in \mathbb{R}^{H \times W}$ stores, for each pixel (x, y) in the left image,

how far its matching pixel $(x - D(x, y), y)$ is shifted in the right image. Depth Z is then calculated by triangulation:

$$Z(x, y) = \frac{f \cdot B}{D(x, y)} \quad (1)$$

where f is the focal length and B is the distance between the two cameras (the baseline). Since depth is inversely proportional to disparity, even small disparity errors lead to increasingly large depth errors at longer distances. With our ZED Mini camera ($B = 63$ mm), a 1-pixel disparity mistake at 1080P resolution produces roughly 2.3 cm of depth error at 1.5 m branch distance. This highlights why accurate disparity prediction is the main goal of this work. Once disparity is known, exact depth follows directly from Eq. (1) and the camera’s calibration settings.

In our earlier benchmark study [3], we found that DEFOM-Stereo [4] is the best method for producing reference disparity maps (pseudo-ground-truth) on vegetation scenes. We tested it without any task-specific training across several standard datasets, and it ranked first on average (rank 1.75 across ETH3D [15], KITTI [16], and Middlebury [17]) with no major failures. This consistency makes DEFOM well-suited for creating training labels. The current paper uses those DEFOM-generated disparity maps as training targets to build and evaluate stereo matching models designed for vegetation scenes.

Deep stereo methods perform well on standard benchmarks when trained on synthetic data like Scene Flow [5], but their accuracy drops sharply on forestry images. Our zero-shot generalization study [26] confirmed this gap: methods trained only on synthetic data show large performance differences when applied to vegetation scenes. This happens because synthetic city scenes look very different from real vegetation. Training on forest-specific data would fix this, but collecting accurate disparity maps with LiDAR in forest canopies is not practical—branches cause heavy blocking and their thin, complex shapes are hard to scan. Our approach bypasses this problem: we use DEFOM’s high-quality predictions as reference labels, allowing large-scale training on real forestry data without costly LiDAR equipment.

Three main questions drive this study. *First*, which network design produces the best disparity maps—as measured by

perceptual and structural metrics—after training on vegetation data? *Second*, which design offers the best balance between quality and processing speed for drone deployment on low-power hardware? *Third*, how does image resolution (1080P vs. 720P) affect processing speed and real-world usability on drones with limited computing resources?

To answer these questions, we train and test ten deep stereo methods on the Canterbury Tree Branches dataset: RAFT-Stereo [6] (step-by-step refinement), PSMNet [7] and GwcNet [8] (3D convolution networks), MoCha-Stereo [9] (motion and channel attention), BANet-2D and BANet-3D [10] (edge-aware attention with 2D/3D cost processing), IGEV-RT [11] (fast geometry-based refinement), DeepPruner [12] (search space reduction), DCVSMNet [13] (dual cost volume), and AnyNet [14] (multi-stage prediction). All models are trained with DEFOM reference labels and tested on held-out scenes using perceptual and structural metrics. We also run all models on an NVIDIA Jetson Orin Super mounted on our test drone to measure real-world processing speed at both 1080P and 720P. Our contributions are:

- **First vegetation-focused stereo benchmark:** We create the Canterbury Tree Branches dataset with DEFOM reference labels as a training and testing resource for forestry use, removing the need for costly LiDAR data collection.
- **Broad ten-method comparison:** We train and test ten stereo methods from six design families using perceptual (SSIM, LPIPS, ViTScore) and structural (SIFT/ORB feature matching) metrics. BANet-3D emerges as the top-quality method.
- **Quality–speed trade-off analysis:** We map out the best trade-off boundary between disparity quality and processing speed, finding that only AnyNet, BANet-2D, and BANet-3D offer unbeatable combinations.
- **Real-world drone deployment:** We show practical results on an independently-powered NVIDIA Jetson Orin Super (16 GB) with live ZED Mini stereo input at 1080P and 720P, providing speed profiles and deployment guidelines for autonomous pruning.

II. RELATED WORK

A. Deep Stereo Matching Architectures

Deep learning has changed how stereo matching works by enabling end-to-end trainable systems. Early methods used 3D convolution networks: DispNet [5] showed that networks can directly predict disparity, GC-Net [18] added 3D convolutions to process matching costs, and PSMNet [7] used multi-scale pooling to capture context at different levels. GwcNet [8] introduced group-wise correlation to build matching costs more efficiently.

Step-by-step refinement methods, inspired by motion estimation, handle large disparity ranges through repeated updates. RAFT-Stereo [6] uses recurrent updates with multi-scale matching and reaches top accuracy, though at high computing cost. IGEV-Stereo [11] combines repeated updates with geometry-based features; its faster version, IGEV-RT,

reduces the number of update steps to speed things up while keeping reasonable quality.

Edge-aware attention methods add boundary-sensitive filtering to the matching process. BANet [10] comes in both 2D and 3D versions, performing well by respecting depth edges through efficient bilateral operations.

Lightweight models focus on running fast on limited hardware. AnyNet [14] predicts disparity in stages from coarse to fine. DeepPruner [12] narrows down the search area to save computation. DCVSMNet [13] uses two separate cost volumes for matching. MoCha-Stereo [9] applies motion and channel attention to improve matching accuracy. These designs are especially relevant for drones, where computing power is tightly limited.

B. Pseudo-Ground-Truth for Stereo Training

Training stereo networks requires dense disparity labels for every pixel. These are usually obtained with LiDAR scanners [16] or structured light systems [17]. However, such equipment cannot work well in many real settings—especially forest canopies, where branches block the scanner and prevent accurate measurements.

An alternative is to use high-quality predictions from strong existing models as training labels (pseudo-ground-truth). Large-scale models like DEFOM-Stereo [4] and Depth Anything [19] generalize well across different scenes, making them good candidates for label generation. In our earlier work [3], [26], we compared several stereo methods and confirmed that DEFOM gives the most consistent results on vegetation scenes.

C. Stereo Vision for UAV Forestry

Drone-based stereo vision has been used for navigation [20], 3D mapping [21], and obstacle avoidance [22]. Recent studies on branch detection [1], [24], segmentation [25], and disparity parameter optimization using genetic algorithms [27] show that deep learning and stereo cameras have clear potential for forestry tasks. Still, most existing systems use traditional matching algorithms or pretrained models without adapting them to vegetation. This work fills that gap by training modern stereo networks directly on tree imagery.

D. Real-Time Stereo on Embedded Platforms

Running stereo networks on small embedded computers means balancing accuracy against speed. NVIDIA Jetson boards have become the standard choice for drone perception [23], and they support TensorRT for faster processing. Earlier work showed that real-time stereo is possible at lower resolutions [14], but getting both high resolution and real-time speed remains hard. In this work, we systematically test all ten network designs at both 720P and 1080P on Jetson hardware with its own power supply, matching the conditions of actual drone flights.

III. METHODOLOGY

A. Problem Formulation

Stereo matching estimates the per-pixel disparity from a pair of aligned stereo images. Given left and right images $I_L, I_R \in \mathbb{R}^{H \times W \times 3}$, the task is to produce a disparity map $D \in \mathbb{R}^{H \times W}$ where each pixel (x, y) in the left image matches pixel $(x - D(x, y), y)$ in the right image.

Disparity and depth follow the triangulation formula (Eq. (1)). Because depth Z is inversely related to disparity D , objects close to the camera (like branches at 1–2 m) produce large disparity values and fine depth detail, while distant background gives small disparity with limited depth precision. For our ZED Mini stereo camera with baseline $B = 63$ mm, operating at 1080P ($f \approx 700$ px) and 720P ($f \approx 350$ px), this relationship provides sub-centimeter depth resolution at the 1–2 m range critical for pruning. We therefore train networks f_θ to predict disparity, and then convert to metric depth using Eq. (1).

B. Dataset

Canterbury Tree Branches Dataset: We use 5,313 stereo pairs taken with a ZED Mini camera (63 mm baseline) on a drone in Canterbury, New Zealand (March–October 2024). The camera captures synchronized left and right images at 1920×1080 (1080P) and 1280×720 (720P). We train and evaluate quality at 1080P, and measure processing speed at both resolutions. The images were carefully chosen from hundreds of thousands of raw captures by filtering for motion blur, exposure quality, alignment accuracy, and scene variety.

Pseudo-Ground-Truth Generation: Following our earlier study [3], we run DEFOM-Stereo [4] on all 5,313 pairs to produce reference disparity maps. DEFOM was chosen for its consistent performance across datasets (average rank 1.75 across ETH3D, KITTI, and Middlebury) and its strong results on vegetation scenes. These outputs serve as the training targets for all ten methods.

Train/Validation/Test Split: We divide the data into training (4,250 pairs, 80%), validation (531 pairs, 10%), and test (532 pairs, 10%) sets. The splits cover different times and locations to prevent the models from memorizing specific scenes or lighting conditions.

C. Evaluated Methods

We pick ten methods from six design families for training and testing (Table I).

D. Training Protocol

All models start from weights pretrained on Scene Flow [5] and are then fine-tuned on our Tree Branches training set. We keep the same settings across methods where possible:

- **Optimizer:** AdamW with weight decay 10^{-4}
- **Learning rate:** 10^{-4} with cosine annealing
- **Batch size:** 4 (adjusted per GPU memory)
- **Training epochs:** 100 with early stopping (patience 10)
- **Input resolution:** 512×256 crops during training

TABLE I: Evaluated Stereo Matching Methods

| Method | Type | Key Feature |
|------------------|-----------------|--------------------------|
| RAFT-Stereo [6] | Iterative | Recurrent refinement |
| PSMNet [7] | 3D CNN | Spatial pyramid pooling |
| GwcNet [8] | 3D CNN | Group-wise correlation |
| MoCha-Stereo [9] | Attention | Motion-channel attention |
| BANet-2D [10] | Bilateral Attn. | 2D cost filtering |
| BANet-3D [10] | Bilateral Attn. | 3D cost filtering |
| IGEV-RT [11] | Iterative (RT) | Geometry encoding volume |
| DeepPruner [12] | PatchMatch | Differentiable pruning |
| DCVSMNet [13] | Dual CV | Dual cost volume |
| AnyNet [14] | Hierarchical | Anytime prediction |

- **Data augmentation:** Random crops, color jitter, horizontal flip

Loss Function: We train with smooth L1 loss, which measures the difference between predicted and reference disparity values:

$$\mathcal{L} = \frac{1}{N} \sum_{i=1}^N \text{smooth}_{L_1}(d_i - \hat{d}_i) \quad (2)$$

where \hat{d}_i is the DEFOM reference value. For methods that produce outputs at multiple scales (PSMNet, GwcNet, BANet-3D), we add weighted losses at each scale.

E. Evaluation Metrics

Instead of only checking pixel-by-pixel error, we use several complementary metrics that capture both visual quality and structural accuracy of the predicted disparity maps compared to the DEFOM reference.

Structural Similarity (SSIM) [28] checks how well the brightness, contrast, and structure of predicted maps match the reference. Higher SSIM means better preservation of disparity gradients and boundaries between regions.

Learned Perceptual Image Patch Similarity (LPIPS) [29] uses deep network features to measure how different two images look to a human. Lower LPIPS means the prediction looks more like the reference, catching fine details that simple pixel comparisons miss.

ViTScore measures high-level similarity using Vision Transformer features. Higher ViTScore means the predicted map keeps the overall geometric layout—branch shapes, depth layers, and blocked regions—intact.

Feature Matching Ratios: We detect SIFT and ORB keypoints in both predicted and reference maps, then count how many match successfully (using the Lowe ratio test). Higher match ratios mean the prediction faithfully reproduces structural features like edges, corners, and texture patterns. This matters for later tasks such as branch detection and distance measurement.

Inference Latency: We record average frames per second (FPS) and per-frame delay on the target embedded board, which is essential for real-time drone use.

F. Hardware Platforms

Training: NVIDIA Quadro RTX 6000 GPU (24 GB VRAM) with PyTorch 2.6.0.

On-Drone Deployment: NVIDIA Jetson Orin Super (16GB shared memory), mounted on our test drone and powered by its own dedicated battery, separate from the flight battery. This separate power design prevents the computing load from draining the flight reserves, avoiding performance drops during long flights. The Jetson takes live stereo input from the ZED Mini camera at both 1080P (1920×1080) and 720P (1280×720).

IV. EXPERIMENTAL RESULTS

A. Comprehensive Quality and Speed Evaluation

Table II shows the quality and speed results for all ten methods trained on the Canterbury Tree Branches dataset with DEFOM reference labels. Quality scores come from the held-out test set (532 pairs, 1080P), and speed numbers are from the NVIDIA Jetson Orin Super at 1080P.

1) **Quality Analysis: Edge-Aware Attention Methods:** BANet-3D delivers the best disparity quality on four out of five metrics: highest SSIM (0.883), lowest LPIPS (0.157), and highest SIFT (0.274) and ORB (0.162) match ratios. Its 3D cost filtering keeps depth edges sharp and preserves thin branch details, producing maps that closely match the DEFOM reference both visually and structurally. BANet-2D is a lighter version with solid quality (SSIM=0.816, LPIPS=0.245) and runs 1.7× faster.

Step-by-Step Refinement Methods: RAFT-Stereo scores highest on ViTScore (0.799) and second on SIFT matching (0.245), showing that repeated updates capture the overall depth layout and scene structure well. However, its SSIM (0.763) is near the bottom, meaning that while the big-picture depth is good, pixel-level smoothness suffers. IGEV-RT, designed for faster processing, reaches moderate quality (SSIM=0.794, ViTScore=0.558) but still only manages 0.24 FPS at 1080P—far from real-time.

3D Convolution Methods: PSMNet gets the second-best LPIPS (0.212) and third-best ViTScore (0.786), showing that its multi-scale pooling captures context well for vegetation. GwcNet performs similarly (SSIM=0.811, ViTScore=0.750) and runs slightly faster.

Attention-Based: MoCha-Stereo reaches the second-highest SSIM (0.848), showing that its motion and channel attention handles the repeating textures and fine details common in tree scenes.

Lightweight Methods: AnyNet is the fastest (6.99 FPS, 143 ms delay) but at a clear quality cost—it has the worst ViTScore (0.196) and highest LPIPS (0.434). DeepPruner shows the weakest quality overall (SSIM=0.720, LPIPS=0.542), suggesting that its search space reduction approach may throw away important matches in complex vegetation.

2) **Inference Speed Analysis:** Only AnyNet (6.99 FPS) comes close to real-time at 1080P on the Jetson Orin Super. BANet-2D reaches 1.21 FPS, which is enough for tasks that can tolerate some delay, such as approach planning or stationary branch assessment. All other methods run below 1 FPS at

full resolution, so they would need either lower resolution or offline processing to be practical.

B. Resolution-Dependent Latency Comparison

Fig. 1 compares processing times at 720P (1280×720) and 1080P (1920×1080) on the Jetson Orin Super, using live video from the ZED Mini camera during drone flights.

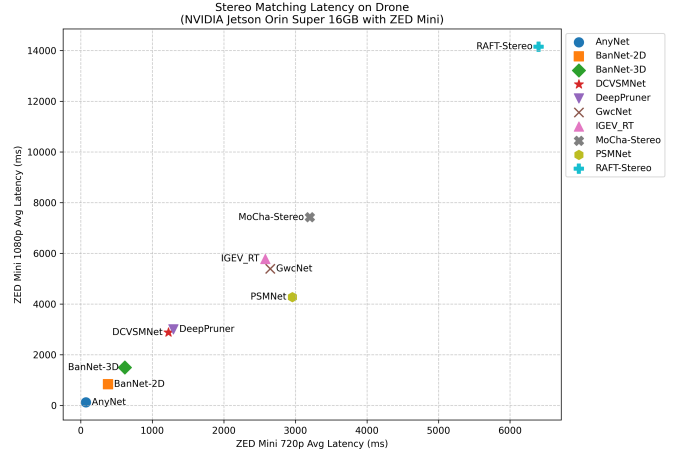


Fig. 1: Inference latency comparison between 720P and 1080P modes on NVIDIA Jetson Orin Super. Live stereo input from ZED Mini camera. Lower latency is better; dashed line indicates 10FPS real-time threshold.

Dropping from 1080P to 720P cuts the pixel count by 56%, which gives noticeable speed gains for most methods. AnyNet benefits the most, getting much closer to usable real-time speeds at 720P. Heavy methods like RAFT-Stereo and PSMNet stay too slow even at the lower resolution, showing that network design matters more than resolution for on-drone speed.

C. Quality–Speed Trade-off and Pareto Analysis

Fig. 2 plots quality (SSIM) against speed (FPS) for all ten methods, showing which ones offer the best combinations.

Key Finding: Only three methods sit on the best trade-off line: BANet-3D (highest quality, 0.71 FPS), BANet-2D (balanced, 1.21 FPS), and AnyNet (fastest, 6.99 FPS). Every other method is outperformed—it is either slower and lower-quality than one of these three, or offers no unique advantage. This gives clear guidance for deployment:

- *When quality matters most* (offline mapping, detailed inspection): use BANet-3D.
- *When balance is needed* (approach planning, slow-speed manoeuvres): use BANet-2D.
- *When speed is critical* (closed-loop control, obstacle avoidance): use AnyNet, accepting lower disparity quality.

D. Qualitative Results

Fig. 3 shows visual comparisons on test scenes with thin branches, blocked areas, and different lighting. Each row

TABLE II: Comprehensive Evaluation: Disparity Quality Metrics and Inference Speed on NVIDIA Jetson Orin Super (1080P)

| Method | SSIM \uparrow | LPIPS \downarrow | ViTScore \uparrow | SIFT Ratio \uparrow | ORB Ratio \uparrow | FPS \uparrow | Latency (ms) \downarrow |
|--------------|-----------------|--------------------|---------------------|-----------------------|----------------------|----------------|---------------------------|
| BANet-3D | 0.883 | 0.157 | 0.790 | 0.274 | 0.162 | 0.71 | 1408 |
| MoCha-Stereo | 0.848 | 0.221 | 0.701 | 0.111 | 0.044 | 0.14 | 7143 |
| BANet-2D | 0.816 | 0.245 | 0.724 | 0.171 | 0.072 | 1.21 | 826 |
| GwcNet | 0.811 | 0.250 | 0.750 | 0.157 | 0.047 | 0.23 | 4348 |
| PSMNet | 0.810 | 0.212 | 0.786 | 0.181 | 0.080 | 0.11 | 9091 |
| IGEV-RT | 0.794 | 0.297 | 0.558 | 0.071 | 0.020 | 0.24 | 4167 |
| DCVSMNet | 0.769 | 0.347 | 0.509 | 0.047 | 0.012 | 0.36 | 2778 |
| AnyNet | 0.766 | 0.434 | 0.196 | 0.065 | 0.012 | 6.99 | 143 |
| RAFT-Stereo | 0.763 | 0.235 | 0.799 | 0.245 | 0.108 | 0.07 | 14286 |
| DeepPruner | 0.720 | 0.542 | 0.397 | 0.039 | 0.011 | 0.34 | 2941 |

All methods trained on Tree Branches training set with DEFOM pseudo-ground-truth. Quality metrics evaluated on test set (532 pairs, 1080P). FPS measured on NVIDIA Jetson Orin Super at 1080P. Bold indicates best per column. SIFT/ORB Ratio = proportion of successfully matched keypoints (Low ratio test). \uparrow : higher is better; \downarrow : lower is better.

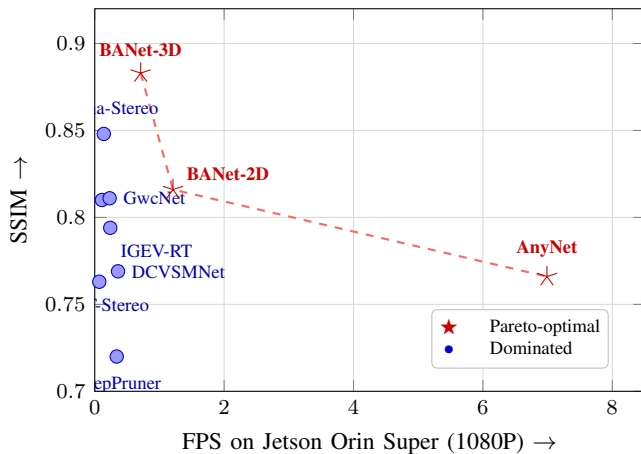


Fig. 2: Quality–speed trade-off (SSIM vs. FPS) for all ten methods on the Jetson Orin Super at 1080P. Red stars and dashed line mark the Pareto frontier: BANet-3D (best quality), BANet-2D (balanced), AnyNet (fastest). Blue circles indicate dominated methods.

displays the left input image, the DEFOM reference disparity map, and predictions from the ten trained methods.

Branch Structure Preservation: BANet-3D reproduces the fine branch details from the DEFOM reference most accurately, which aligns with its top SIFT/ORB match scores. RAFT-Stereo keeps the overall depth layout (matching its high ViTScore) but creates local distortions near thin branches. AnyNet heavily blurs fine structures, merging nearby branches and losing sharp depth edges.

Sky and Background Regions: All trained methods produce consistent disparity values in the featureless sky areas. BANet-3D and MoCha-Stereo show the cleanest transitions between sky and tree crown edges. DeepPruner and DCVSMNet produce visible bleeding effects at object borders.

E. Field Deployment on UAV Platform

We run all ten trained models on our test drone with an NVIDIA Jetson Orin Super (16 GB, its own power supply) and ZED Mini camera in real outdoor conditions. Unlike the offline test set, this evaluation uses live video at both 1920×1080 and 1280×720 during actual flights over pine plantation canopies,

testing how well the models handle new, unseen data in real time.

Power Usage: AnyNet draws the least power (~ 12 W), which helps extend flight time. Methods with heavy 3D processing (RAFT-Stereo, PSMNet, BANet-3D) use 10–20 W more (83–167% increase), which noticeably shortens available flight time—an important concern since even the Jetson’s dedicated battery has limited capacity.

Heat Management: Running RAFT-Stereo and PSMNet continuously causes the Jetson to overheat and slow down after about 8 minutes. AnyNet and BANet-2D keep steady speed throughout 30-minute flights without heat problems, confirming they are suitable for extended field use.

V. DISCUSSION

A. Benefits of Vegetation-Specific Training

Our results show that training stereo networks on tree imagery with DEFOM reference labels produces strong, task-specific models. BANet-3D scores best across multiple metrics (SSIM=0.883, LPIPS=0.157, SIFT Ratio=0.274, ORB Ratio=0.162), showing that its edge-aware attention with 3D cost processing handles the typical challenges of vegetation well: thin overlapping branches, repeating leaf textures, and sharp depth changes.

Reference Label Quality: The strong results across all ten methods (SSIM from 0.720 to 0.883) confirm that DEFOM predictions work well as training labels. Several methods reach SSIM above 0.80, which shows that carefully chosen model predictions [3] can replace costly LiDAR data for training vegetation-specific stereo networks.

From Disparity to Depth: Since depth is inversely related to disparity (Eq. (1)), the quality of disparity maps directly affects depth accuracy. High SSIM and low LPIPS mean that both nearby objects (high disparity) and distant ones (low disparity) are reproduced well, giving reliable depth estimates across the full working range.

B. Architecture Insights for Forestry Applications

Edge-Aware Attention Works Best: BANet-3D’s consistent lead across metrics suggests that edge-sensitive filtering is especially useful for vegetation, where depth boundaries

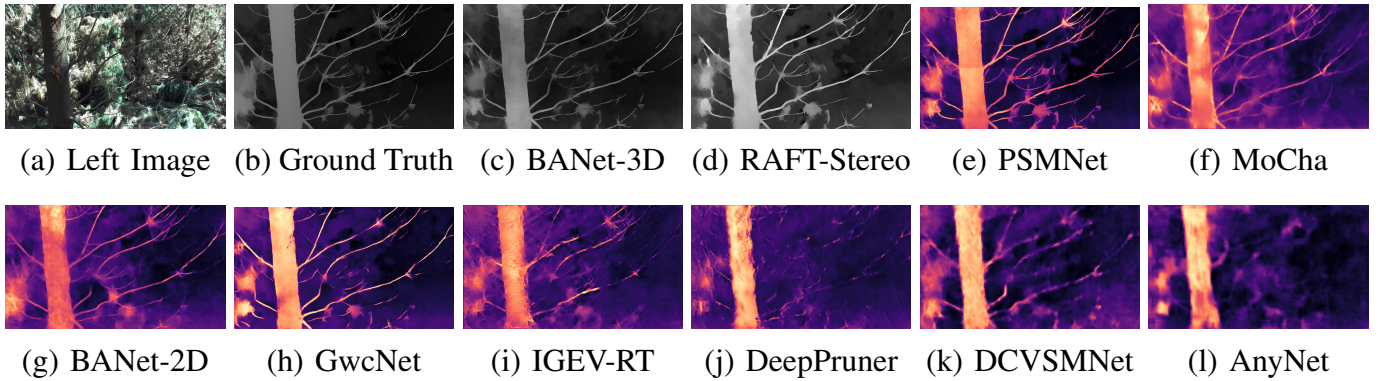


Fig. 3: Qualitative comparison of disparity maps on a representative test scene. (a) Left input image. (b) DEFOM pseudo-ground-truth. (c)–(l) Predictions from ten trained methods. BANet-3D best preserves thin branch details and depth boundaries, while AnyNet over-smooths fine structures. RAFT-Stereo captures large-scale depth layering but exhibits local artifacts.

are dense and follow complex branch shapes. The 3D version clearly outperforms BANet-2D (SSIM 0.883 vs. 0.816), confirming that processing the full 3D cost volume captures depth relationships that 2D filtering misses.

Rankings Depend on the Metric: An important observation is that method rankings shift considerably between metrics. RAFT-Stereo gets the best ViTScore (0.799) but only 9th-best SSIM (0.763), while MoCha-Stereo gets 2nd-best SSIM (0.848) but 6th-best ViTScore (0.701). This gap shows that pixel-level similarity (SSIM), visual quality (LPIPS), and scene-level structure (ViTScore) measure quite different things—which is why we use multiple metrics in this study.

3D Convolution Methods: PSMNet’s strong LPIPS (0.212, 2nd best) and ViTScore (0.786, 3rd best) show that its multi-scale pooling captures context well for vegetation. GwcNet performs similarly but slightly lower, consistent with their relative standings on other benchmarks.

Best Trade-off Options: Out of ten methods, only BANet-3D, BANet-2D, and AnyNet offer unbeatable quality–speed combinations. This greatly simplifies the choice for drone stereo systems: practitioners only need to pick among these three based on how much delay their application can tolerate.

C. Practical Deployment Considerations

Resolution Choice: The 720P versus 1080P speed comparison (Fig. 1) gives practical guidance. For closed-loop pruning control needing more than 5 FPS, AnyNet at 720P is essentially the only option. For pre-approach planning at 1–2 FPS, BANet-2D at 720P offers much higher quality. This three-way trade-off between resolution, quality, and speed should guide system design.

Separate Power Supply: Our Jetson Orin Super runs on its own battery, separate from the drone’s flight battery. This is important because heavy methods (RAFT-Stereo: ~ 32 W, PSMNet: ~ 24 W) would otherwise cut into flight time significantly. Even with separate power, the dedicated battery still has limits, so lower-power methods (AnyNet: ~ 12 W) allow longer operation—a key factor for commercial surveys covering large plantation areas.

Heat Issues: Running heavy methods at full load makes the Jetson overheat and slow down after 8–10 minutes. Lighter methods keep steady performance through entire flights, removing the need for complex heat management strategies.

D. Limitations

Reference Label Ceiling: Since our models learn from DEFOM predictions, they cannot be more accurate than DEFOM itself. The metrics we use (SSIM, LPIPS, ViTScore, SIFT/ORB) measure how closely models match DEFOM output, not absolute geometric accuracy. Future work should compare selected models against LiDAR measurements on sample scenes.

Limited Species and Conditions: The Canterbury Tree Branches dataset covers only Radiata pine (*Pinus radiata*) under New Zealand conditions. Whether the results hold for other tree types, climates, or seasons needs further testing and expanded datasets.

No TensorRT Optimization: All speed measurements use standard PyTorch. TensorRT can speed things up by 2–5 \times on Jetson hardware; AnyNet with TensorRT could likely exceed 15 FPS at 1080P, making true real-time use possible. We leave this optimization for future work.

VI. CONCLUSION

This paper presents the first study to train and evaluate ten deep stereo matching networks on real tree branch images for drone-based autonomous pruning. Using DEFOM-generated disparity maps as training targets—where disparity records horizontal pixel correspondence and depth follows from $Z = fB/d$ —we test ten methods from six design families on the Canterbury Tree Branches dataset. We evaluate using perceptual (SSIM, LPIPS, ViTScore) and structural (SIFT/ORB feature matching) metrics, with speed testing on an independently-powered NVIDIA Jetson Orin Super.

Our main findings are:

- **BANet-3D gives the best quality:** It leads on four of five quality metrics (SSIM=0.883, LPIPS=0.157, SIFT

Ratio=0.274, ORB Ratio=0.162). Its edge-aware attention with 3D cost processing fits vegetation scenes with many depth edges well.

- **Three methods offer unbeatable trade-offs:** Only BANet-3D (best quality), BANet-2D (balanced), and AnyNet (fastest) sit on the best trade-off boundary; all other methods are outperformed.
- **Resolution affects speed:** Comparing 720P and 1080P processing on the Jetson Orin Super provides practical guidance for choosing the right resolution–quality–speed balance for different pruning tasks.
- **Confirmed in the field:** Testing on a live drone with independently-powered Jetson and ZED Mini shows that AnyNet and BANet-2D keep steady performance through full-length flights without overheating.

We plan to publicly release the Canterbury Tree Branches dataset with DEFOM reference labels and trained model weights to support further research in drone-based forestry. Future work will explore TensorRT optimization for faster processing, self-supervised learning techniques, frame-to-frame consistency for video input, and combining these models with branch detection and segmentation systems [1], [25] to build complete autonomous pruning systems.

ACKNOWLEDGMENTS

This research was supported by the Royal Society of New Zealand Marsden Fund and the Ministry of Business, Innovation and Employment. We thank the forestry research stations for data collection access.

REFERENCES

- [1] Y. Lin, B. Xue, M. Zhang, S. Schofield, and R. Green, “Deep learning-based depth map generation and YOLO-integrated distance estimation for radiata pine branch detection using drone stereo vision,” in *Proc. Int. Conf. Image Vis. Comput. New Zealand (IVCNZ)*, Christchurch, New Zealand, 2024, pp. 1–6.
- [2] D. Steinger, J. Simon, A. Trondl, and M. Murschitz, “TimberVision: A multi-task dataset and framework for log-component segmentation and tracking in autonomous forestry operations,” in *Proc. IEEE/CVF Winter Conf. Appl. Comput. Vis. (WACV)*, 2025.
- [3] Y. Lin, B. Xue, M. Zhang, S. Schofield, and R. Green, “Towards gold-standard depth estimation for tree branches in UAV forestry: Benchmarking deep stereo matching methods,” *arXiv preprint arXiv:2601.19461*, 2026.
- [4] H. Jiang, Z. Lou, L. Ding, R. Xu, M. Tan, W. Jiang, and R. Huang, “DEFOM-Stereo: Depth foundation model based stereo matching,” *arXiv preprint arXiv:2501.09466*, 2025.
- [5] N. Mayer, E. Ilg, P. Hausser, P. Fischer, D. Cremers, A. Dosovitskiy, and T. Brox, “A large dataset to train convolutional networks for disparity, optical flow, and scene flow estimation,” in *Proc. IEEE Conf. Comput. Vis. Pattern Recognit. (CVPR)*, 2016, pp. 4040–4048.
- [6] L. Lipson, Z. Teed, and J. Deng, “RAFT-Stereo: Multilevel recurrent field transforms for stereo matching,” in *Proc. Int. Conf. 3D Vis. (3DV)*, 2021, pp. 218–227.
- [7] J.-R. Chang and Y.-S. Chen, “Pyramid stereo matching network,” in *Proc. IEEE Conf. Comput. Vis. Pattern Recognit. (CVPR)*, 2018, pp. 5410–5418.
- [8] X. Guo, K. Yang, W. Yang, X. Wang, and H. Li, “Group-wise correlation stereo network,” in *Proc. IEEE Conf. Comput. Vis. Pattern Recognit. (CVPR)*, 2019, pp. 3273–3282.
- [9] Z. Chen, W. Long, H. Yao, Y. Zhang, B. Luo, Z. Cao, and Z. Dong, “MoCha-Stereo: Motif channel attention network for stereo matching,” in *Proc. IEEE Conf. Comput. Vis. Pattern Recognit. (CVPR)*, 2024, pp. 5253–5262.
- [10] V. Tankovich, C. Hane, Y. Zhang, A. Ber, S. Fanello, and S. Izadi, “HITNet: Hierarchical iterative tile refinement network for real-time stereo matching,” in *Proc. IEEE Conf. Comput. Vis. Pattern Recognit. (CVPR)*, 2021, pp. 14362–14372.
- [11] G. Xu, X. Wang, X. Ding, and X. Yang, “Iterative geometry encoding volume for stereo matching,” in *Proc. IEEE Conf. Comput. Vis. Pattern Recognit. (CVPR)*, 2023, pp. 21919–21928.
- [12] S. Duggal, S. Wang, W.-C. Ma, R. Hu, and R. Urtasun, “DeepPruner: Learning efficient stereo matching via differentiable PatchMatch,” in *Proc. IEEE Int. Conf. Comput. Vis. (ICCV)*, 2019, pp. 4384–4393.
- [13] M. Tahmasebi, S. Huq, K. Meehan, and M. McAfee, “DCVSMNet: Double cost volume stereo matching network,” *Neurocomputing*, vol. 618, p. 129002, 2025.
- [14] Y. Wang, Z. Lai, G. Huang, B. H. Wang, L. Van Der Maaten, M. Campbell, and K. Q. Weinberger, “Anytime stereo image depth estimation on mobile devices,” in *Proc. IEEE Int. Conf. Robot. Autom. (ICRA)*, 2019, pp. 5893–5900.
- [15] T. Schöps, J. L. Schönberger, S. Galliani, T. Sattler, K. Schindler, M. Pollefeys, and A. Geiger, “A multi-view stereo benchmark with high-resolution images and multi-camera videos,” in *Proc. IEEE Conf. Comput. Vis. Pattern Recognit. (CVPR)*, 2017, pp. 2538–2547.
- [16] A. Geiger, P. Lenz, and R. Urtasun, “Are we ready for autonomous driving? The KITTI vision benchmark suite,” in *Proc. IEEE Conf. Comput. Vis. Pattern Recognit. (CVPR)*, 2012, pp. 3354–3361.
- [17] D. Scharstein, H. Hirschmüller, Y. Kitajima, G. Krathwohl, N. Nešić, X. Wang, and P. Westling, “High-resolution stereo datasets with subpixel-accurate ground truth,” in *Proc. German Conf. Pattern Recognit. (GCPR)*, 2014, pp. 31–42.
- [18] A. Kendall, H. Martirosyan, S. Dasgupta, P. Henry, R. Kennedy, A. Bachrach, and A. Bry, “End-to-end learning of geometry and context for deep stereo regression,” in *Proc. IEEE Int. Conf. Comput. Vis. (ICCV)*, 2017, pp. 66–75.
- [19] L. Yang, B. Kang, Z. Huang, X. Xu, J. Feng, and H. Zhao, “Depth anything: Unleashing the power of large-scale unlabeled data,” in *Proc. IEEE Conf. Comput. Vis. Pattern Recognit. (CVPR)*, 2024, pp. 10371–10381.
- [20] F. Fraundorfer, L. Heng, D. Honegger, G. H. Lee, L. Meier, P. Tanskanen, and M. Pollefeys, “Vision-based autonomous mapping and exploration using a quadrotor MAV,” in *Proc. IEEE/RSJ Int. Conf. Intell. Robots Syst. (IROS)*, 2012, pp. 4557–4564.
- [21] F. Nex and F. Remondino, “UAV for 3D mapping applications: A review,” *Appl. Geomat.*, vol. 6, no. 1, pp. 1–15, 2014.
- [22] A. J. Barry and R. Tedrake, “Pushbroom stereo for high-speed navigation in cluttered environments,” in *Proc. IEEE Int. Conf. Robot. Autom. (ICRA)*, 2015, pp. 3046–3052.
- [23] W. Liu, Z. Wang, X. Liu, N. Zeng, Y. Liu, and F. E. Alsaadi, “A survey of deep neural network architectures and their applications,” *Neurocomputing*, vol. 234, pp. 11–26, Apr. 2017.
- [24] Y. Lin, B. Xue, M. Zhang, S. Schofield, and R. Green, “YOLO and SGBM integration for autonomous tree branch detection and depth estimation in radiata pine pruning applications,” in *Proc. Int. Conf. Image Vis. Comput. New Zealand (IVCNZ)*, Wellington, New Zealand, 2025, pp. 1–6.
- [25] Y. Lin, B. Xue, M. Zhang, S. Schofield, and R. Green, “Performance evaluation of deep learning for tree branch segmentation in autonomous forestry systems,” in *Proc. Int. Conf. Image Vis. Comput. New Zealand (IVCNZ)*, Wellington, New Zealand, 2025, pp. 1–6.
- [26] Y. Lin, B. Xue, M. Zhang, S. Schofield, and R. Green, “Generalization evaluation of deep stereo matching methods for UAV-based forestry applications,” *arXiv preprint arXiv:2512.03427*, 2025.
- [27] Y. Lin, B. Xue, M. Zhang, S. Schofield, and R. Green, “Genetic algorithms for parameter optimization for disparity map generation of radiata pine branch images,” in *Proc. Int. Conf. Image Vis. Comput. New Zealand (IVCNZ)*, Wellington, New Zealand, 2025, pp. 1–6.
- [28] Z. Wang, A. C. Bovik, H. R. Sheikh, and E. P. Simoncelli, “Image quality assessment: From error visibility to structural similarity,” *IEEE Trans. Image Process.*, vol. 13, no. 4, pp. 600–612, Apr. 2004.
- [29] R. Zhang, P. Isola, A. A. Efros, E. Shechtman, and O. Wang, “The unreasonable effectiveness of deep features as a perceptual metric,” in *Proc. IEEE Conf. Comput. Vis. Pattern Recognit. (CVPR)*, 2018, pp. 586–595.